

CHEMISTRY

A European Journal

A Journal of



Accepted Article

Title: Push-pull (iso)quinoline chromophores: synthesis, photophysical properties, and use for white light emission.

Authors: Zaina Ibrahim Mohamed Allaoui, Estelle le Gall, Arnaud Fihey, Rodrigo Plaza-Pedroche, Claudine Katan, Françoise Robin-le Guen, Julián Rodríguez-López, and Sylvain Achelle

This manuscript has been accepted after peer review and appears as an Accepted Article online prior to editing, proofing, and formal publication of the final Version of Record (VoR). This work is currently citable by using the Digital Object Identifier (DOI) given below. The VoR will be published online in Early View as soon as possible and may be different to this Accepted Article as a result of editing. Readers should obtain the VoR from the journal website shown below when it is published to ensure accuracy of information. The authors are responsible for the content of this Accepted Article.

To be cited as: *Chem. Eur. J.* 10.1002/chem.202000817

Link to VoR: <http://dx.doi.org/10.1002/chem.202000817>

Supported by
ACES

WILEY-VCH

Push-pull (iso)quinoline chromophores: synthesis, photophysical properties, and use for white light emission.

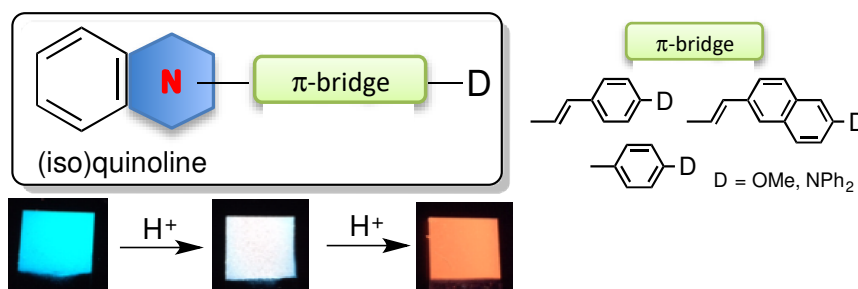
Zaina Ibrahim Mohamed Allaoui,^[a] Estelle le Gall,^[b] Arnaud Fihey,^[a]
Rodrigo Plaza-Pedroche,^[c] Claudine Katan,^[a] Françoise Robin-le Guen,^[a]
Julián Rodríguez-López,^{*,[c]} and Sylvain Achelle^{*,[a]}

^[a] Université de Rennes, CNRS, Institut des Sciences Chimiques de Rennes - UMR 6226, F 35000 Rennes, France; E-mail: sylvain.achelle@univ-rennes1.fr

^[b] IUT de Lannion, Université de Rennes 1, Rue Édouard Branly, F 22300 Lannion, France.

^[c] Área de Química Orgánica, Facultad de Ciencias y Tecnologías Químicas, Universidad de Castilla-La Mancha, Avda. Camilo José Cela 10, 13071 Ciudad Real, Spain; E-mail: julian.rodriguez@uclm.es

Graphical abstract



Abstract. The photophysical properties of a series of conjugated push-pull (iso)quinolines have been studied. The compounds were synthesized by well-established and straightforward methodologies. The materials exhibited not only emission solvatochromism in a variety of non-polar solvents, but also tunable halochromism. Some of the compounds remained moderately luminescent after protonation and these had a red emissive form, which was used to obtain white light emission, both in solution and in thin film, by the controlled protonation of the initially blue-green emitting materials. This methodology has potential applications in white OLED fabrication with two forms of a single emitter in equilibrium.

Keywords: (iso)quinolines; fluorescence; white-light emission; push-pull chromophores.

INTRODUCTION

Conjugated push-pull chromophores based on azaheterocyclic fragments have been intensively investigated in recent years.^{1,2,3,4,5} Indeed, the photophysical properties of these materials can be easily tuned by environmental stimuli such as polarity,^{6,7,8,9} pH,^{8-10,11} or the presence of metal cations.¹² Six-membered nitrogen heterocycles such as pyridine,^{6,13} quinoline³ or (benzo)diazines¹⁻⁵ act as moderate-to-strong electron-withdrawing groups. When protons or metal cations are added the photophysical properties are modified due to the interaction with the electron lone pair of the nitrogen atoms of the heterocycle. Such engagement of the electron lone pair leads to an increase in the electron-withdrawing character and enhances the intramolecular charge transfer (ICT) into the chromophore.¹⁴ This phenomenon has been used to obtain sensors^{10,11} and a variety of optical switches.^{15,16,17} The protonation of azaheterocyclic push-pull chromophores generally leads to a bathochromic effect on the absorption spectrum.^{8,9,14} However, the effect is less predictable for the emission. Quenching is generally observed but in some cases a red shift accompanied by either an increase or decrease in the intensity can be obtained.⁸

There is currently great interest in obtaining white light emission.¹⁸ Pure white light was defined in 1931 by the Commission Internationale de l'Eclairage (CIE) and it corresponds to CIE chromaticity coordinates of (0.33, 0.33). White light can be obtained by a combination of red, green and blue emitters in the appropriate proportions or by mixing any other two complementary lights.¹⁸ Independent fluorophores are typically employed, but a new strategy based on an equilibrium between two different forms of the same material has been proposed. The two forms should emit complementary colors and can consist of monomer/excimer,^{19,20,21} neutral/(de)protonated species,^{14,22,23,24} or free/complexed ligand.^{24,25}

We recently described methoxy-substituted arylvinylpyrimidine derivatives that emit blue light in their neutral form and red light upon protonation.^{26,27} A mixture of the two forms

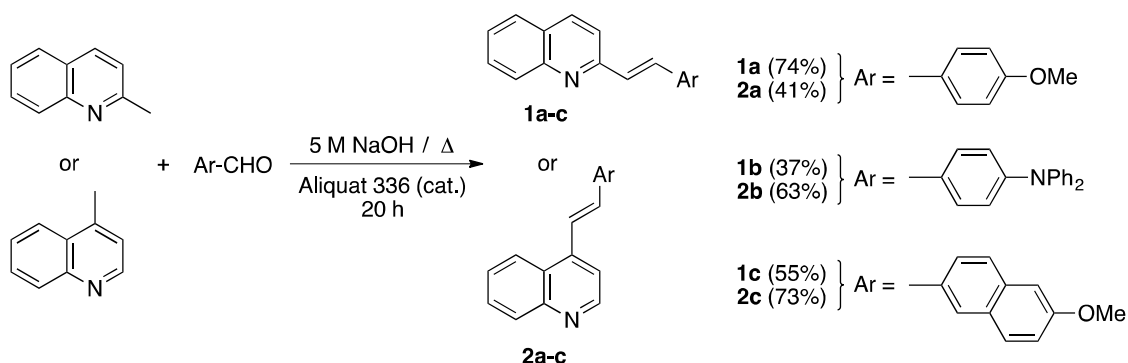
in a precise proportion provided white light both in solution and in thin films. Analogously, a mixture of purple-emitting carbazole-substituted pyrimidines and their yellow emitting protonated forms also afforded white light emission.²⁸ Unfortunately, it was found that the low basicity of the pyrimidine ring ($pK_a \approx 1.1$) precludes the fabrication of stable white light emitting thin films, particularly when a volatile acid such as trifluoroacetic acid is used. Pyridine derivatives have the advantage of stronger basicity ($pK_a \approx 5.2$). Nevertheless, the pyridine ring has a weaker electron-withdrawing character and stronger electron-donating fragments are required as part of the π -conjugated push-pull structure (e.g., a diphenylamino group). Although white luminescence could be obtained with this type of chromophore in solution, the blue-shifted emission of both the neutral and protonated forms in solid state precluded white emission.²⁹

The quinoline ring is a stronger electron-withdrawing group than the pyridine ring and it has a slightly less basic character ($pK_a \approx 4.8\text{--}4.9$).³⁰ Several triphenylamine-substituted quinolines have been reported to show red-shifted luminescence upon protonation.^{31,32} Accordingly, we focused our efforts on investigating conjugated push-pull (iso)quinoline derivatives. In this contribution, the synthesis of a series of such (iso)quinoline chromophores is described and their photophysical properties are reported. The luminescence behavior upon protonation with the aim of achieving white light emission both in solution and solid state is also presented.

RESULTS AND DISCUSSION

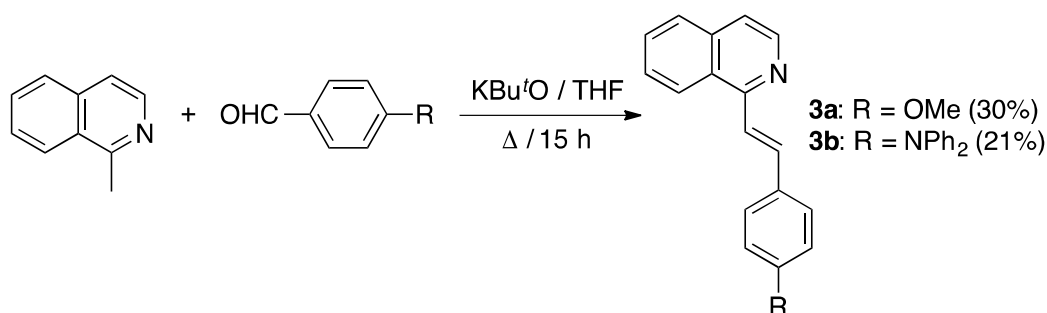
Synthesis. 2- and 4-Arylvinylquinolines **1** and **2** were obtained by Knoevenagel condensation of 2- and 4-methylquinoline, respectively, with the appropriate aldehyde. Reactions were carried out according to a previously reported protocol using boiling aqueous 5 M NaOH as solvent and Aliquat[®] 336 as a phase-transfer catalyst.³³ Two equivalents of

methylquinoline were employed in order to avoid the presence of unreacted aldehyde. Compounds **1** and **2** were obtained in moderate to good yield (Scheme 1).



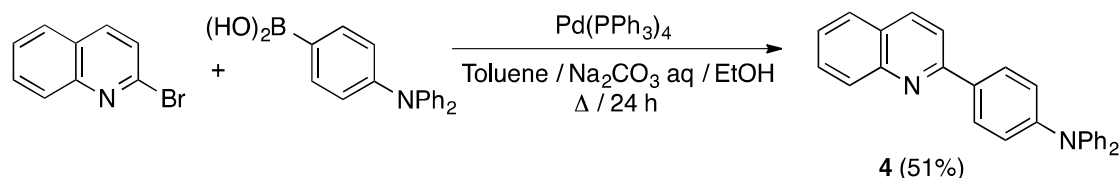
Scheme 1. Synthesis of 2- and 4-arylvinylquinolines **1** and **2**.

These conditions were not efficient when 1-methylisoquinoline was used as the starting material. In this case, a stronger base, i.e., potassium *tert*-butoxide (KBu^tO) in refluxing THF, was required to form the 1-styrylisoquinolines **3** in low yield (Scheme 2). In all cases, compounds **1–3** were selectively obtained with *trans*-configured vinylenes bridges, as commonly observed in the Knoevenagel condensation of methylazaheterocycles.³⁴ It should be noted that the synthesis of 3-arylvinylisoquinolines by this methodology proved unsuccessful regardless of the base used (aqueous NaOH, KBu^tO , dimsyl potassium), and the starting 3-methylisoquinoline was recovered.



Scheme 2. Synthesis of 1-styrylisoquinolines **3**.

The 2-arylquinoline **4** was prepared in moderate yield by Suzuki–Miyaura cross-coupling reaction of 2-bromoquinoline with 4-(diphenylamino)phenylboronic acid under classical conditions (Scheme 3).



Scheme 3. Synthesis of 2-[4-(diphenylamino)phenyl]quinoline (**4**).

The above compounds were perfectly stable in the solid state and could be stored without special precautions. The compounds were highly soluble in common organic solvents, e.g., dichloromethane, chloroform and THF. The structure and purity of each compound was unequivocally established by NMR spectroscopy. The observed $^3J(\text{H,H})$ coupling constants of ~16 Hz for the vinylic protons confirmed the *trans* configuration of the double bond. All previously unreported materials were also characterized by high resolution mass spectrometry (HRMS).

UV-vis and fluorescence spectroscopy in solution. The UV-vis and photoluminescence (PL) spectroscopic data for compounds **1–4**, registered in CHCl_3 at room temperature, are presented in Table 1. Low concentration solutions ($1.0\text{--}4.0 \times 10^{-5}$ M) were used to avoid aggregation and self-absorption effects. *Trans* to *cis* isomerization was not observed under the analysis conditions.

As an example, the spectra of compounds **1b**, **2b** and **3b** are provided in Figure 1. All compounds exhibited structureless absorption and emission bands with rather large Stokes shifts in the $4900\text{--}6300\text{ cm}^{-1}$ range, which is associated with highly polarizable π -conjugated systems due to intramolecular charge transfer (ICT).³⁵ It is worth noting that 4-arylvinylquinolines **2** presented higher Stokes shifts than their analogs **1** and **3**. As expected,

the presence of strong electron-donating diphenylamino groups resulted in significantly red-shifted absorption and emission maxima as well as higher Stokes shifts in each series. With the exception of compound **1c**, the methoxy-substituted derivatives were poorly emissive ($\Phi_F \leq 0.02$). Diphenylamino substituted compounds **1–3b** and **4** exhibited blue-green emission with emission maxima increasing in the order: **4** << **1b** < **3b** < **2b**. The 2-arylquinoline **4**, without a vinylene linker, showed an outstanding fluorescence quantum yield (0.98), which is significantly higher than that of its 2-arylvinyl analog **1b**. This phenomenon has been observed previously in other series of compounds.^{4,36} The quantum yield for 2-styrylquinoline **1b** ($\Phi_F = 0.61$) was also substantially higher than those for the 4-styrylquinoline **2b** and the 1-styrylisoquinoline **3b** ($\Phi_F = 0.29$ in both cases).

Table 1. UV-vis and photoluminescence (PL) data for compounds **1–4** in CHCl_3 solution.

Compd ^a	λ_{abs} (nm)	ϵ ($\text{mM}^{-1} \text{cm}^{-1}$)	λ_{em} (nm)	Φ_F	Stokes Shift (cm^{-1})
1a	346	16.4	417	0.02	4921
1b	399	37.9	502	0.61	5142
1c	354	24.9	430	0.15	4993
2a	347	17.7	429	< 0.01	5508
2b	397	21.0	519	0.29	6285
2c	354	16.2	450	0.02	6026
3a	360	17.1	441	< 0.01	5102
3b	402	25.4	512	0.29	5344
4	374	24.7	462	0.98	5093

^a All spectra were recorded at room temperature at $c = 1.25\text{--}1.89 \times 10^{-5}$ M.

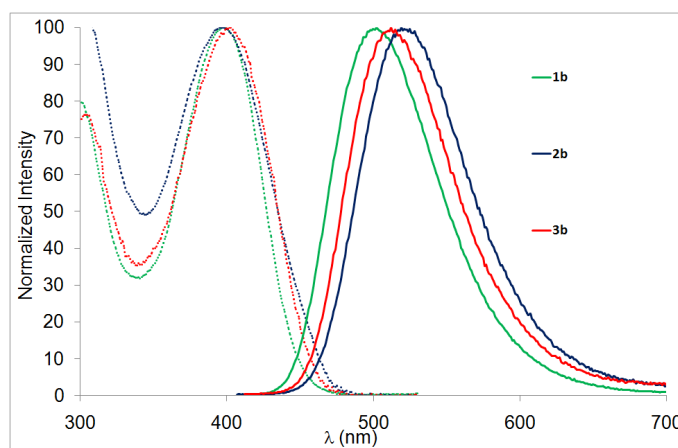


Figure 1. Normalized absorption (dashed lines) and emission (solid lines) spectra of compounds **1b** (green), **2b** (blue) and **3b** (red) in CHCl_3 solution.

Solvatochromic behavior. Emission solvatochromism is one of the possible ways to evaluate ICT. Push-pull chromophores generally exhibit a limited absorption solvatochromism and a large positive fluorosolvatochromism, i.e., a red shift is observed when the solvent polarity is increased due to the stabilization of a highly polar excited state.^{35,37,38} Therefore, the emission properties of compounds **1–4** were studied in a variety of aprotic solvents of increasing polarity. The results are summarized in Table 2. As representative examples, the normalized spectra registered for **3b** are shown in Figure 2 (see Figure S1 in the Supporting Information for other compounds). The emission maxima, expressed as wavenumber, were plotted *versus* the $E_T(30)$ Dimroth–Reichardt polarity parameters³⁹ and in all cases a good linearity was observed (Figure 3 and Figure S2). Regarding the diphenylamino series, the absolute value of the slope of the regression line is somewhat higher for the 4-styrylquinoline **2b**, which indicates a stronger ICT. Spectra broadening could also be observed when the polarity was increased. Nevertheless, there is a no clear correlation between the full width at half maximum (FWHM) expressed as difference of wavenumber and $E_T(30)$ (Table S1, Supporting Information).

Table 2. Emission solvatochromism of compounds **1–4** in various aprotic solvents.

Compd	<i>n</i> -Heptane (30.9) ^a	Toluene (33.9) ^a	1,4-Dioxane (36.0) ^a	THF (37.4) ^a	CHCl ₃ (39.1) ^a	CH ₂ Cl ₂ (40.7) ^a	Acetone (42.2) ^a	MeCN (45.6) ^a
1a	390	400	402	409	417	419	421	433
1b	448	466	471	495	502	513	517	544
1c	399	410	412	427	430	434	437	448
2a	411	424	425	433	429	437	445	454
2b	451	480	487	519	529	538	550	569
2c	418	434	430	447	450	454	459	465
3a	425	434	438	444	441	451	449	453
3b	460	479	480	511	512	521	528	549
4	410	430	437	458	462	474	480	499

^a $E_T(30)$ Dimroth–Reichardt polarity parameter in kcal mol^{−1}.

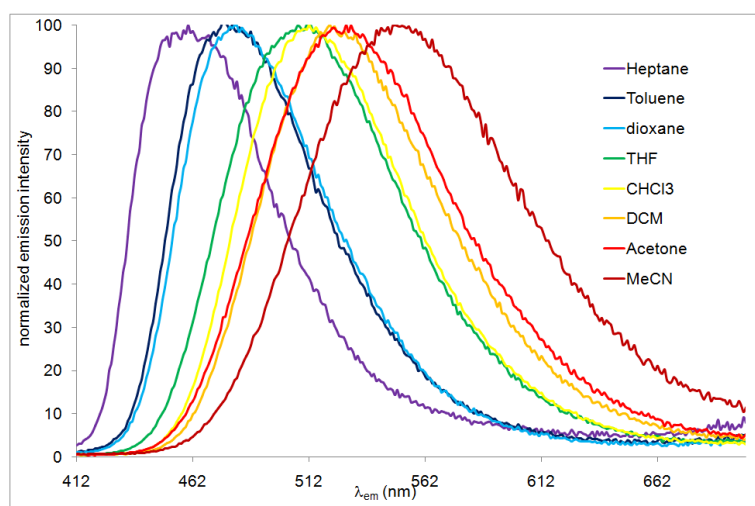


Figure 2. Normalized emission spectra of **3b** in different aprotic solvents.

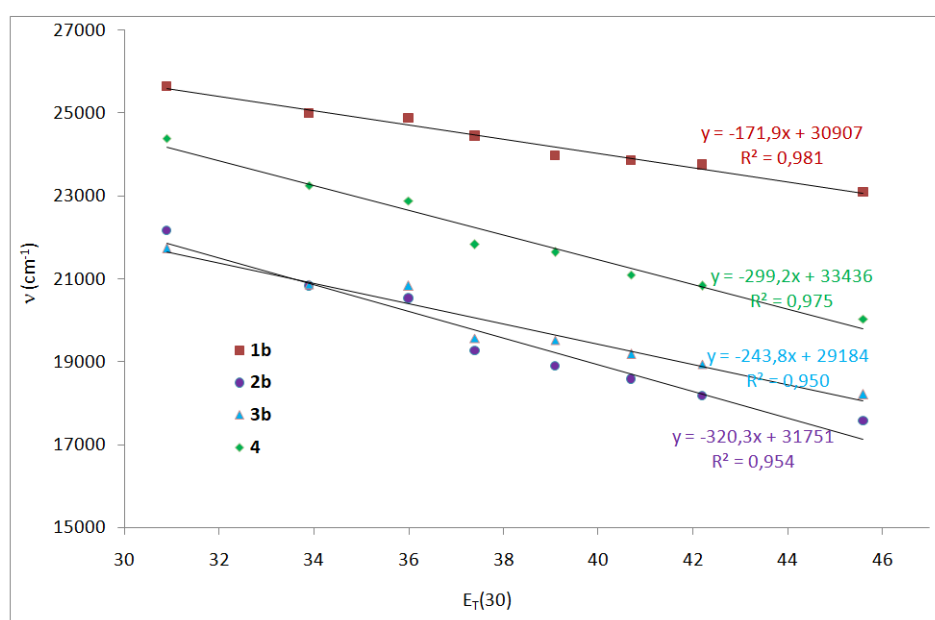


Figure 3. Emission maxima (ν_{em}) for compounds **1–3b** and **4** (diphenylamino series) as a function of the $E_T(30)$ Dimroth–Reichardt polarity parameters.

Protonation studies. The consequences of protonation on the photophysical properties of the materials were studied in a 10^{-2} M solution of camphorsulfonic acid (CSA) in chloroform. The results are given in Table 3 and the normalized absorption and emission spectra of the neutral and protonated form of **1b** are shown in Figure 4. In all cases a significant red shift in the absorption and emission bands was observed. Whereas the methoxystyryl derivatives **1–3a** remained poorly emissive after protonation, the emission

quantum yield of the methoxynaphthylvinyl derivatives **1c** and **2c** increased. The diphenylaminostyryl derivatives **1–3b** remained moderately emissive and afforded red-light, although a noticeable decrease in the quantum yield was observed for all of these materials. The fluorescence intensity of compound **4** decreased dramatically in the presence of CSA, as reported previously for other acids.³¹

Table 3. UV-vis and PL data of compounds **1–4** in acid solution (10^{-2} M CSA in CHCl_3).

Compd ^a	λ_{abs} (nm)	ϵ ($\text{mM}^{-1} \text{cm}^{-1}$)	λ_{em} (nm)	Φ_{F}	Stokes Shift (cm^{-1})
1a	412	25.0	502	0.04	4352
1b	509	52.3	660	0.18	4495
1c	428	18.3	541	0.31	4880
2a	412	21.9	505	< 0.01	4470
2b	509	17.3	672	0.22	4765
2c	427	14.8	545	0.08	5071
3a	413	17.5	513	< 0.01	4720
3b	512	23.8	674	0.20	4694
4	467	31.9	650	0.03	6029

^a All spectra were recorded at room temperature at $c = 1.25\text{--}1.89 \times 10^{-5}$ M.

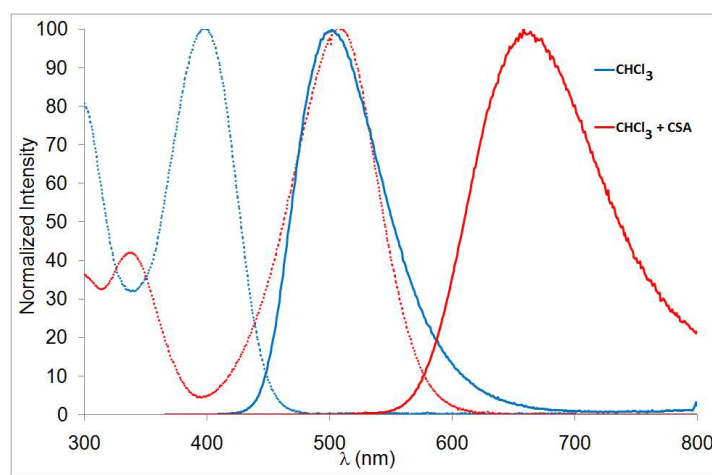


Figure 4. Normalized absorption (dashed lines) and emission (solid lines) of compound **1b** in CHCl_3 with (red) or without (blue) CSA (10^{-2} M).

The changes observed for compound **1b** in the UV-vis and emission spectra upon addition of CSA are shown in Figure 5. The increase in the concentration of acid led to the

progressive attenuation of the charge transfer absorption band and the appearance of a new red-shifted band corresponding to the protonated species. An isosbestic point, which is characteristic of an equilibrium between two species, was observed at ~440 nm (Figure 5, left). A similar trend was observed for the fluorescence response: the addition of CSA also caused a steady decrease of the emission band of the neutral form and the enhancement of a new red-shifted band for the protonated form with an isoemissive point (Figure 5, right). Both bands exhibited a similar intensity when 0.6–0.7 equivalents of CSA were added, at an excitation wavelength of 440 nm. Similar behaviors were also found for compounds **1c**, **2b** and **3b** (see Figures S3–S5 in the Supporting Information). Fine tuning of the band ratio was possible by changing the excitation wavelength (see Figure S6 in the Supporting Information). In a similar way to pyrimidine and pyridine derivatives,²⁶⁻²⁹ the coexistence of neutral and protonated forms of **1b**, **1c**, **2b** and **3b** in solution led to emission rather close to white light (Figure 6, see also Figures S7–S9 in the Supporting Information). The calculated CIE chromaticity coordinates are listed in Table 4.

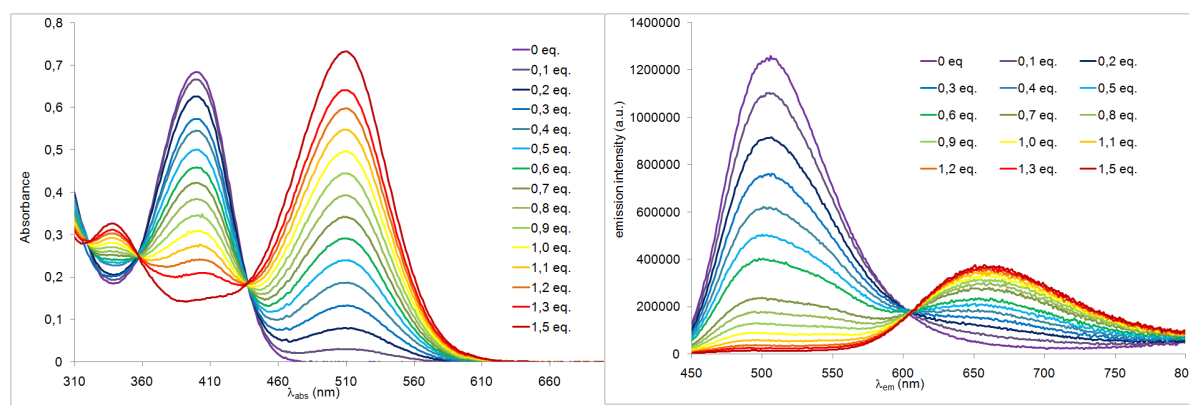


Figure 5. Changes in the absorption (left) and emission (right, $\lambda_{\text{exc}} = 440$ nm) spectra of a CHCl_3 solution of **1b** ($c = 1.89 \times 10^{-5}$ M) upon addition of CSA (0–1.5 equivalents).

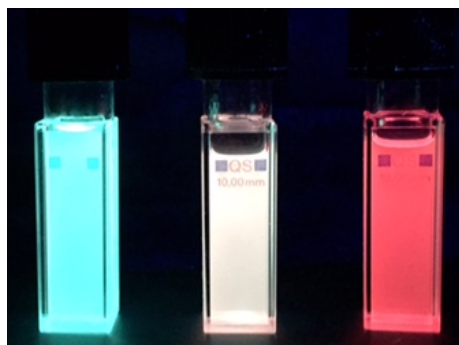


Figure 6. Changes in the color of a CHCl_3 solution of **1b** ($c = 1.89 \times 10^{-5} \text{ M}$) after the addition of 0.9 equivalents (middle) and in 10^{-2} M CSA (right). Photographs were taken in the dark upon irradiation with a hand-held UV lamp ($\lambda_{\text{em}} = 366 \text{ nm}$).

Table 4. CIE coordinates in CHCl_3 solution ($c = 1.0\text{--}2.0 \times 10^{-5} \text{ M}$).

Compd	Chromaticity coordinates (x,y)		
	Neutral form	Protonated form	Mixture of neutral and protonated forms
1b	(0.23, 0.50)	(0.62, 0.35)	(0.31, 0.47) ^a
1c	(0.15, 0.09)	(0.36, 0.57)	(0.26, 0.34) ^b
2b	(0.32, 0.57)	(0.64, 0.34)	(0.40, 0.51) ^a
2c	(0.07, 0.13)	(0.39, 0.57)	-
3b	(0.28, 0.55)	(0.62, 0.36)	(0.36, 0.51) ^a
4	(0.15, 0.16)	(0.61, 0.39)	-

^a 0.5 equivalents of CSA, $\lambda_{\text{exc}} = 440 \text{ nm}$. ^b 0.3 equivalents of CSA, $\lambda_{\text{exc}} = 385 \text{ nm}$.

Theoretical studies. Calculations based on Density Functional Theory (DFT) and its time-dependent extension (TD-DFT) were performed on a selection of chromophores (**1b**, **2b**, **3b** and **4**) to gain a deeper understanding of the relation between molecular structure and photophysical properties. As expected for this class of chromophore, all compounds exhibited a lowest-energy transition (see Table 6) with non-negligible charge transfer character, which is reasonably well described by the frontier molecular orbitals HOMO and LUMO (Figure S27 and S28). Geometry optimizations of the neutral forms revealed that whereas **1b** and **3b** are already planar in their ground state, **2b** and **4** have a molecular backbone with a significant twist angle in the ground state (27° and 19° , respectively) that vanishes in the excited state,

thus undergoing significant structural reorganization in their excited state. The latter process can be further captured through the variation of the bond length alternation (BLA), which is summarized in Table 5 for the three compounds that have a vinyl bridge. For the neutral forms, BLA are sizeable and consistent with the significant Stokes shift observed experimentally (Table 1) and confirmed theoretically (Table 6). Clearly, **2b** has the largest Stokes shift as a result of largest structural reorganization between its ground and excited states. With regards to the protonated forms, the BLA variation between the ground and excited states of each compound (Table 5) is significantly smaller when compared to that of their neutral counterparts. This in turn leads to markedly smaller Stokes shifts for the protonated species. Interestingly, whereas the protonated form of **2b** is almost planar in the ground state, protonated **3b** becomes twisted, probably due to the greater steric hindrance produced by the proton and its counter anion, and the Stokes shift is comparable to that of **2b**. Among all computed excited state geometries, the protonated form of compound **4** is the only one that retains a significant twist angle in the excited state (13° as compared to 25° in the ground state). This is probably related to steric hindrance as a result of the missing vinyl moiety between the phenyl and quinoline rings. The remaining twist may favor non-radiative relaxation pathways and may be responsible for the very low radiative quantum yield measured experimentally (Table 3).

Table 5. Computed Bond Length Alternation (BLA [\AA] of the C–C=C–C vinyl bridge for the neutral and protonated compounds **1b–3b** in CHCl_3 (see computational details in the Experimental Part).

Compd	BLA [\AA] ^a			
	Neutral form		Protonated form	
	GS	ES	GS	ES
1b	0.1112	0.0050	0.0669	0.0215
2b	0.1108	–0.0009	0.0660	0.0248
3b	0.1111	0.0007	0.0707	0.0181

^a GS is the ground state and ES is the excited state.

Table 6. Theoretical absorption and emission data for neutral and protonated compounds **1b–3b** and **4** in CHCl₃ with a linear response PCM model and state-specific (SS) values in parenthesis.

Compd	λ_{abs} (nm)	f^a	λ_{em} (nm)	f^a	Stokes Shift (cm ⁻¹)
1b	371 (SS: 384)	1.64	456 (SS: 454)	1.90	5024 (SS: 4015)
2b	376 (SS: 398)	1.30	485 (SS: 481)	1.56	5977 (SS: 4336)
3b	388 (SS: 398)	1.37	486 (SS: 474)	1.56	5197 (SS: 4029)
4	341 (SS: 362)	1.01	399 (SS: 424)	1.30	4264 (SS: 4039)
1b-H⁺	476 (SS: 441)	1.80	543 (SS: 497)	1.93	2592 (SS: 2555)
2b-H⁺	505 (SS: 464)	1.53	573 (SS: 516)	1.68	2350 (SS: 2172)
3b-H⁺	486 (SS: 452)	1.47	568 (SS: 514)	1.65	2970 (SS: 2669)
4b-H⁺	425 (SS: 413)	1.12	499 (SS: 506)	1.14	3489 (SS: 4450)

^a f is the oscillator strength.

Photophysical properties in thin film. Simple thin films of polystyrene doped with 1 wt% of the diphenylamino-substituted derivatives **1–3b** were prepared by spray deposition on glass substrates. The films remained luminescent and exhibited blue emission, although the emission maxima experienced a blue shift when compared to the CHCl₃ solutions. The addition of 0.06 equivalents of CSA to the solutions of **1b** and **2b** and 0.18 equivalents to the solution of **3b** used for the spray deposition resulted in a film that exhibited two emission bands with CIE coordinates close to pure white (Figure 7, Table 5). Films of fully protonated compounds led to emission maxima in the orange-red region. It is worth noting that the color coordinates changed slightly when different areas of the films were irradiated, which can be attributed to the inhomogeneities of the deposited layers. These significant changes in the emission colors could be easily followed by the naked eye (Figure 7, see also Figures S10 and S11 in the Supporting Information).

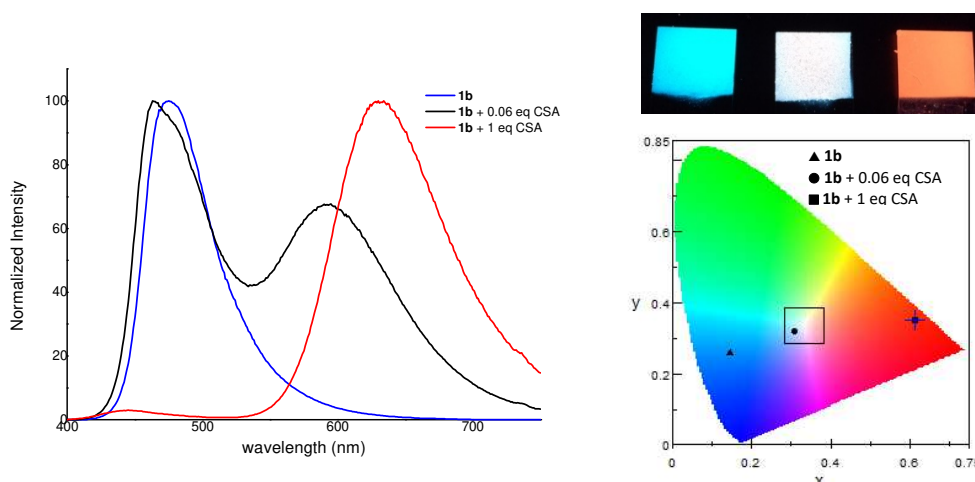


Figure 7. Fluorescence spectra ($\lambda_{\text{exc}} = 366$ nm), colors and CIE chromaticity diagram for polystyrene thin films doped with **1b** (1 wt%) in the absence and the presence of 0.06 and 1 equivalents of CSA (from left to right). Photographs were taken in the dark upon irradiation with a hand-held UV lamp ($\lambda_{\text{em}} = 366$ nm).

Table 5. PL data and CIE coordinates of thin films of polystyrene doped with 1%wt **1–3b**.

Compd	λ_{em} (nm)		Chromaticity coordinates (x,y)		
	Neutral form	Protonated form	Neutral form	Protonated form	Mixture of neutral and protonated forms
1b	475	632	(0.15, 0.26)	(0.61, 0.35)	(0.31, 0.32) ^a
2b	479	625	(0.16, 0.29)	(0.58, 0.35)	(0.33, 0.36) ^a
3b	481	628	(0.15, 0.31)	(0.56, 0.33)	(0.34, 0.33) ^b

^a 0.06 equivalents of CSA, $\lambda_{\text{exc}} = 366$ nm. ^b 0.18 equivalents of CSA, $\lambda_{\text{exc}} = 366$ nm.

CONCLUSION

We have designed a series of conjugated push-pull (iso)quinolines that proved to be effective materials for white light emission. Well-known methodologies based on the Knoevenagel condensation and Suzuki–Miyaura reaction were used for the synthesis of these compounds, in which either a methoxy or diphenylamino donor group was connected to the (iso)quinoline acceptor fragment through different π -bridges. The study of the photophysical properties revealed significant red shifts in the absorption and emission maxima on increasing the electron-donating ability of the substituent, which is explained on the basis of an enhanced ICT and confirmed by a stronger emission solvatochromism. The presence of diphenylamino

groups also led to higher Stokes shifts and fluorescence quantum yields in each series. The molecules could be easily protonated at the nitrogen atom of the (iso)quinoline fragment. Protonation provided a substantial enhancement in the electron-withdrawing character and, consequently, the appearance of a new red-shifted complementary emitting band. Albeit with a noticeable decrease in the quantum yield, diphenylaminostyryl derivatives **1–3b** remained moderately emissive after the addition of acid. Thus, white light emission could be obtained by controlled protonation both in solution and in solid state. This is a new example of the use of a single emitting material with two forms of complementary emitting colors as a new strategy to obtain white light.

EXPERIMENTAL PART

General information. All solvents were reagent grade for synthesis and spectroscopic grade for photophysical measurements. The starting materials were purchased from Sigma-Aldrich or TCI and were used without further purification. For air- and moisture-sensitive reactions, all glassware was flame-dried and cooled under nitrogen. NMR spectra were recorded in CDCl₃ on Bruker Avance 300 (¹H at 300 MHz and ¹³C at 75 MHz) and Bruker Avance Neo 500 (¹H at 500 MHz) spectrometers. The chemical shifts δ are reported in ppm and are referenced to the residual protons of the deuterated solvent or carbon nuclei (¹H, δ = 7.27 ppm; ¹³C, δ = 77.0 ppm). The coupling constants J are given in Hz. In the ¹H NMR spectra, the following abbreviations are used to describe the peak patterns: s (singlet), d (doublet), dd (doublet of doublets), t (triplet), m (multiplet). In the ¹³C NMR spectra, the nature of the carbons (C, CH, CH₂ or CH₃) was determined by performing a JMOD experiment. Acidic impurities in CDCl₃ were removed by treatment with solid K₂CO₃. Melting points (°C) were measured on a Kofler hot-stage with a precision of 2 degrees (\pm 2 °C). High-resolution mass analyses were performed at the 'Centre Régional de Mesures Physiques de l'Ouest' (CRMPO,

Université de Rennes 1) using a Bruker MicroTOF-Q II apparatus. Analytical thin layer chromatography (TLC) was performed on silica gel plates (Merck 60 F254) and compounds were visualized by irradiation with UV light at 254 and 365 nm. Flash chromatography was performed using silica Acros SI 60 (60–200 mesh ASTM). UV-visible and fluorescence spectroscopy studies in solution were conducted on a Spex Fluoromax-3 Jobin-Yvon Horiba spectrophotometer. Compounds were excited at their absorption maxima (band of lowest energy) to record the emission spectra. All solutions were measured with optical densities below 0.1. Fluorescence quantum yields ($\pm 10\%$) were determined relative to 9,10-bis(phenylethynyl)anthracene in cyclohexane ($\Phi_F = 1.00$). Acidic impurities in solvents were removed by treatment with Al_2O_3 . Stokes shifts were calculated considering the lowest energetic absorption band. Thin films were prepared by the direct nebulization of CHCl_3 solutions of polystyrene doped with the appropriate compound (1 wt%, in the absence and the presence of CSA) on various heated glass substrates through a fine spray nozzle obtained by using an air compressor system. Fluorescence spectra of these films were recorded on a Jasco FP-8300 spectrofluorometer at $\lambda_{\text{exc}} = 366$ nm.

General procedure for the synthesis of arylvinylquinoline derivatives. A stirred mixture of the corresponding methylquinoline (2 mmol) and the appropriate aldehyde (1 mmol) in aqueous sodium hydroxide (5 M, 10 mL) containing Aliquat[®] 336 (22 mg, 0.05 mol) was heated under reflux for 20 h. The mixture was cooled and the precipitate was filtered off and washed with water. For compounds **1** and **2c**, the precipitate was washed with acidified (HCl) ethanol, solubilized in CH_2Cl_2 and a few drops of NEt_3 were added to neutralize the formed quinolinium salt. The organic solution was washed with water, dried with MgSO_4 , and the solvent was evaporated under reduced pressure.

(E)-2-(4-Methoxystyryl)quinoline (1a). Cream solid, yield 74% (195 mg). Mp 124–126 °C (lit.⁴⁰: 125–127 °C). ^1H NMR (300 MHz, CDCl_3): δ 8.11 (d, $J = 8.7$ Hz, 1H), 8.06 (d, $J = 8.4$

Hz, 1H), 7.77 (d, $J = 8.1$ Hz, 1H), 7.72–7.56 (m, 5H), 7.51–7.45 (m, 1H), 7.29 (d, $J = 16.5$ Hz, 1H), 6.94 (d, $J = 8.7$ Hz, 2H), 3.85 (s, 3H). The spectroscopic data were consistent with those reported in the literature.³⁹

(E)-2-[4-(Diphenylamino)styryl]quinoline (1b). Orange solid, yield 37% (146 mg). Mp 150–152 °C (lit.³²: 150–151.4 °C). ¹H NMR (300 MHz, CDCl₃): δ 8.11 (d, $J = 8.7$ Hz, 1H), 8.07 (d, $J = 8.7$ Hz, 1H), 7.76 (d, $J = 8.1$ Hz, 1H), 7.72–7.64 (m, 2H), 7.62 (d, $J = 16.2$ Hz, 1H), 7.52–7.45 (m, 3H), 7.32–7.26 (m, 5H), 7.17–7.12 (m, 4H), 7.08–7.04 (m, 4H). The spectroscopic data were consistent with those reported in the literature.³²

(E)-2-[2-(6-Methoxynaphthalen-2-yl)vinyl]quinoline (1c). Cream solid, yield 55% (171 mg). Mp 150 °C (dec.). ¹H NMR (300 MHz, CDCl₃): δ 8.11 (d, $J = 8.7$ Hz, 1H), 8.09 (d, $J = 8.7$ Hz, 1H), 7.93–7.67 (m, 8H), 7.53–7.47 (m, 1H), 7.47 (d, $J = 16.2$ Hz, 1H), 7.18–7.15 (m, 2H), 3.94 (s, 3H). ¹³C NMR and JMOD (75 MHz, CDCl₃): δ 55.4 (CH₃), 106.0 (CH), 119.2 (CH), 119.3 (CH), 124.3 (CH), 126.1 (CH), 127.3 (CH), 127.3 (C), 127.5 (CH), 127.9 (CH), 128.3 (CH), 129.0 (C), 129.2 (CH), 129.7 (CH), 129.8 (CH), 132.0 (C), 134.7 (CH), 134.8 (C), 136.3 (CH), 148.3 (C), 156.3 (C), 158.2 (C). HRMS (ESI/ASAP, TOF): m/z calcd for C₂₂H₁₈NO [M + H]⁺ 312.1383, found 312.1387.

(E)-4-(4-Methoxystyryl)quinoline (2a). Purified by column chromatography (SiO₂, petroleum ether/EtOAc, 1/1). Pale yellow solid, yield 41% (144 mg). Mp 90–92 °C. ¹H NMR (300 MHz, CDCl₃): δ 8.87 (d, $J = 4.8$ Hz, 1H), 8.20 (d, $J = 7.8$ Hz, 1H), 8.13 (d, $J = 7.8$ Hz, 1H), 7.72–7.53 (m, 6H), 7.27 (d, $J = 16.2$ Hz, 1H), 6.94 (d, $J = 8.7$ Hz, 2H), 3.84 (s, 3H). ¹³C NMR and JMOD (75 MHz, CDCl₃): δ 55.4 (CH₃), 114.3 (CH), 116.7 (CH), 120.4 (CH), 123.5 (CH), 126.4 (CH), 128.5 (CH), 129.3 (CH), 129.4 (C), 130.0 (CH), 134.7 (CH), 143.3 (C), 148.6 (C), 150.1 (CH), 160.3 (C). HRMS (ESI/ASAP, TOF): m/z calcd for C₁₈H₁₆NO [M + H]⁺ 262.1226, found 262.1231.

(E)-4-[4-(Diphenylamino)styryl]quinoline (2b). Purified by column chromatography (SiO₂, petroleum ether/EtOAc, 1/1). Orange solid, yield 63% (229 mg). ¹H NMR (300 MHz, CDCl₃): δ 8.87 (d, *J* = 4.8 Hz, 1H), 8.22 (d, *J* = 8.4 Hz, 1H), 8.13 (d, *J* = 8.4 Hz, 1H), 7.76–7.70 (m, 1H), 7.71 (d, *J* = 16.5 Hz, 1H), 7.61–7.55 (m, 2H), 7.50 (d, *J* = 8.7 Hz, 2H), 7.33–7.27 (m, 5H), 7.16–7.05 (m, 8H). ¹³C NMR and JMOD (75 MHz, CDCl₃): δ 116.7 (CH, 120.6 (CH), 122.9 (CH), 123.5 (CH), 124.5 (CH), 124.9 (CH), 126.4 (CH), 126.4 (C), 128.1 (CH), 129.3 (CH), 129.4 (CH), 130.1 (CH), 130.3 (C), 134.6 (CH), 143.3 (C), 147.3 (C), 148.5 (C), 148.7 (C) 150.2 (CH). HRMS (ESI/ASAP, TOF): *m/z* calcd for C₂₉H₂₃N₂ [M + H]⁺ 399.1856, found 399.1855.

(E)-4-[2-(6-Methoxynaphthalen-2-yl)vinyl]quinoline (2c). Pale yellow solid, yield 73% (225 mg). Mp 110–112 °C. ¹H NMR (300 MHz, CDCl₃): δ 8.92 (d, *J* = 4.5 Hz, 1H), 8.28 (d, *J* = 8.1 Hz, 1H), 8.14 (d, *J* = 8.4 Hz, 1H), 7.93–7.73 (m, 6H), 7.72–7.58 (m, 2H), 7.49 (d, *J* = 15.9 Hz, 1H), 7.20–7.17 (m, 2H), 3.95 (s, 3H). ¹³C NMR and JMOD (75 MHz, CDCl₃): δ 55.4 (CH₃), 106.0 (CH), 116.9 (CH), 119.4 (CH), 121.9 (CH), 123.5 (CH), 124.1 (CH), 126.4 (C), 126.5 (CH), 127.5 (CH), 127.8 (CH), 129.0 (C), 129.3 (CH), 129.8 (CH), 130.1 (CH), 131.9 (C), 134.8 (C), 135.3 (CH), 143.2 (C), 148.7 (C), 150.2 (CH), 158.3 (C). HRMS (ESI/ASAP, TOF): *m/z* calcd for C₂₂H₁₈NO [M + H]⁺ 312.1383, found 312.1385.

General procedure for the synthesis of arylvinylisoquinoline derivatives. 1-Methylisoquinoline (143 mg, 1 mmol) and the corresponding aldehyde (1 mmol) were dissolved in anhydrous THF (15 mL). K⁺Bu[–]O (447 mg, 4 mmol) was slowly added at room temperature and the solution was heated under reflux for 15 h. After cooling, water was added, the THF was evaporated, and the mixture was extracted with CH₂Cl₂. The organic layer was dried over MgSO₄ and the solvent was removed under vacuum. The crude product was purified by flash chromatography (SiO₂, petroleum ether/EtOAc, 7/3).

(E)-1-(4-Methoxystyryl)isoquinoline (3a). Pale yellow solid, yield 30% (75 mg). Mp 88–90 °C. ^1H NMR (300 MHz, CDCl_3): δ 8.54 (d, $J = 5.7$ Hz, 1H), 8.37 (d, $J = 8.4$ Hz, 1H), 7.96 (d, $J = 15.6$ Hz, 1H), 7.87 (d, $J = 15.6$ Hz, 1H), 7.82 (d, $J = 8.7$ Hz, 1H), 7.70–7.59 (m, 4H), 7.54 (d, $J = 5.7$ Hz, 1H), 6.95 (d, $J = 8.7$ Hz, 2H), 3.85 (s, 3H). ^{13}C NMR and JMOD (75 MHz, CDCl_3): δ 55.4 (CH_3), 114.2 (CH), 119.6 (CH), 120.6 (CH), 124.5 (CH), 126.6 (C), 127.1 (CH), 127.3 (CH), 128.8 (CH), 129.7 (C), 129.8 (CH), 135.4 (CH), 136.8 (C), 142.5 (CH), 150.2 (CH), 154.9 (C), 160.1 (C). HRMS (ESI/ASAP, TOF): m/z calcd for $\text{C}_{18}\text{H}_{16}\text{NO}$ $[\text{M} + \text{H}]^+$ 262.1226, found 262.1229.

(E)-1-[4-(Diphenylamino)styryl]isoquinoline (3b). Yellow solid, yield 21% (81 mg). ^1H NMR (500 MHz, CDCl_3): δ 8.55 (d, $J = 5.5$ Hz, 1H), 8.37 (d, $J = 8.0$ Hz, 1H), 7.96 (d, $J = 15.5$ Hz, 1H), 7.89 (d, $J = 15.5$ Hz, 1H), 7.83 (d, $J = 8.5$ Hz, 1H), 7.70–7.67 (m, 1H), 7.64–7.61 (m, 1H), 7.58 (d, $J = 9.0$ Hz, 2H), 7.55 (d, $J = 5.5$ Hz, 1H), 7.31–7.28 (m, 4H), 7.16 (dd, $J = 8.5$ Hz, $J = 1.0$ Hz, 4H), 7.10–7.06 (m, 4H). ^{13}C NMR and JMOD (75 MHz, CDCl_3): δ 119.6 (CH), 120.7 (CH), 122.9 (CH), 123.4 (CH), 124.5 (CH), 124.8 (CH), 126.7 (C), 127.1 (CH), 127.3 (CH), 128.4 (CH), 129.4 (CH), 129.8 (CH), 130.7 (C), 135.4 (CH), 136.7 (C), 142.5 (CH), 147.4 (C), 148.3 (C), 154.8 (C). HRMS (ESI/ASAP, TOF): m/z calcd for $\text{C}_{29}\text{H}_{23}\text{N}_2$ $[\text{M} + \text{H}]^+$ 399.1856, found 399.1858.

2-[4-(Diphenylamino)phenyl]quinoline (4). A stirred mixture of the corresponding 2-bromoquinoline (208 mg, 1 mmol), 4-(diphenylamino)phenylboronic acid (433 mg, 1.5 mmol) and $\text{Pd}(\text{PPh}_3)_4$ (68 mg, 0.06 mmol) in degassed aqueous 2 M sodium carbonate (2 mmol, 1 mL)/ethanol (1 mL)/toluene (15 mL) was heated under reflux for 24 h under a nitrogen atmosphere. The reaction mixture was cooled, filtered and EtOAc/water 1/1 (20 mL) was added. The organic layer was separated and the aqueous layer was extracted with additional EtOAc (2×10 mL). The combined organic extracts were dried over MgSO_4 and the solvent was evaporated under reduced pressure. The crude product was purified by flash

chromatography (SiO₂, CH₂Cl₂). Yellow solid, yield 51% (191 mg). Mp 174–176 °C (lit.⁴¹: 172–174 °C). ¹H NMR (300 MHz, CDCl₃): δ 8.17 (d, J = 8.7 Hz, 1H), 8.16 (d, J = 8.4 Hz, 1H), 8.06 (d, J = 8.7 Hz, 2H), 7.83 (d, J = 8.4 Hz, 1H), 7.81 (d, J = 8.1 Hz, 1H), 7.72 (m, 1H), 7.50 (m, 1H), 7.33–7.26 (m, 4H), 7.24–7.18 (m, 6H), 7.11–7.06 (m, 2H). The spectroscopic data were consistent with those reported in the literature.⁴¹

Computational details. All calculations were performed with the Gaussian 16 code.⁴² Geometry optimizations for the different compounds were followed by frequency calculations, to ensure the true nature of the energy minimum, at the PBE0⁴³/6-311+G(d,p) level. To obtain the absorption features Time-Dependent DFT calculations were performed at this ground state equilibrium geometry in a vertical fashion using the CAM-B3LYP⁴⁴ and the 6-311+G(d,p) basis set, while the excited-state geometries were optimized with the same level of theory to provide the emission properties. Bond Length Alternation (BLA) values were computed for the ground state and excited state on the C–C=C–C vinyl bridge as a difference between the mean value of the two simple bond distances and the double bond one.

In all of these steps the solvent effects were included through the Polarizable Continuum Model (PCM).⁴⁵ For absorption and emission vertical transitions, both the non-equilibrium Linear-Response⁴⁶ (LR) PCM and the State-Specific⁴⁷ (SS) PCM were used for the sake of comparison. Note that for emission, only the final vertical transition, at the excited state equilibrium geometry, was computed at the SS-PCM level, while the equilibrium LR-PCM was used for the excited state relaxation process.

Acknowledgments. J. R.-L. thanks the Ministerio de Economía y Competitividad/Agencia Estatal de Investigación/FEDER for financial support (project CTQ2017-84561-P). Funding from the Junta de Comunidades de Castilla-La Mancha/FEDER is also gratefully acknowledged by J. R.-L. and S. A. (project SBPLY/17/180501/000214).

REFERENCES

-
- ¹ S. Achelle, C. Baudequin, N. Plé, *Dyes Pigm.* **2013**, 98, 575-600.
- ² G. N. Lipunova, E. V. Nosova, V. N. Charushin, O. N. Chupakhin, *Curr. Org. Synth.* **2018**, 15, 793-814.
- ³ E. V. Nosova, S. Achelle, G. N. Lipunova, V. N. Charushin, O. N. Chupakhin, *Russ. Chem. Rev.* **2019**, 88, 1128-1178.
- ⁴ S. Achelle, J. Rodríguez-López, F. Robin-le Guen, *ChemistrySelect* **2018**, 3, 1852-1886.
- ⁵ R. Komatsu, H. Sasabe, J. Kido, *J. Photon. Energy* **2018**, 8, 032108.
- ⁶ H. Agnihotri, A. K. Vasu, V. Palakollu, S. Kanvah, *Photochem. Photobiol. Sci.* **2015**, 14, 2159-2167.
- ⁷ J. Rodríguez-Aguilar, M. Vidal, C. Pastenes, C. Aliaga, M. C. Rezende, M. Domínguez, *Photochem. Photobiol.* **2018**, 94, 1100-1108.
- ⁸ S. Achelle, J. Rodríguez-López, F. Bureš, F. Robin-le Guen, *Chem. Rec.* **2019**, DOI: 10.1002/rcr.201900064.
- ⁹ V. Schmitt, S. Moschel, H. Detert, *Eur. J. Org. Chem.* **2013**, 5665-5669.
- ¹⁰ R. Tang, X. Wang, W. Zhang, X. Zhuang, S. Bi, W. Zhang, F. Zhang, *J. Mater. Chem. C* **2016**, 4, 7640-7648.
- ¹¹ Z. Yang, W. Qin, J. W. Y. Lam, S. Chen, H. H. Y. Sung, I. D. Williams, B. Z. Tang, *Chem. Sci.* **2013**, 4, 3725-3730.
- ¹² C. Hadad, S. Achelle, I. López-Solera, J. García-Martínez, J. Rodríguez-López, *Dyes Pigm.* **2013**, 97, 230-237.

- ¹³ K. Melánová, D. Cvejn, F. Bureš, V. Zima, J. Svoboda, L. Beneš, T. Mikysek, O. Pytela, P. Knotek, *Dalton Trans.* **2014**, 43, 10462-10470.
- ¹⁴ D. Liu, Z. Zhang, H. Zhang, Y. Wang, *Chem. Commun.* **2013**, 49, 10001-10003.
- ¹⁵ E. Cariati, C. Dragonetti, E. Lucenti, F. Nisic, S. Righetto, D. Roberto, E. Tordin, *Chem. Commun.* **2014**, 50, 1608-1610.
- ¹⁶ E. Cariati, C. Botta, S. G. Danelli, A. Forni, A. Giaretta, U. Giovanella, E. Lucenti, D. Marinotto, S. Righetto, R. Ugo, *Chem. Commun.* **2014**, 50, 14225-14228.
- ¹⁷ E. Lucenti, A. Forni, D. Marinotto, A. Previtali, S. Righetto, E. Cariati, *Inorganics* **2019**, 7, 38.
- ¹⁸ S. Mukherjee, P. Thilagar, *Dyes Pigm.* **2014**, 110, 2-27.
- ¹⁹ S. Tao, Y. Zhou, C.-S. Lee, S.-T. Lee, D. Huang, X. Zhang, *J. Mater. Chem.* **2008**, 18, 3981-3984.
- ²⁰ L. Liu, F. Chen, B. Xu, Y. Dong, Z. Zhao, W. Tian, L. Ping, *Synth. Met.* **2010**, 160, 1968-1972.
- ²¹ T. Fleetham, J. Ecton, Z. Wang, N. Bakken, J. Li, *Adv. Mater.* **2013**, 25, 2573-2576.
- ²² H. V. Huynh, X. He, T. Baumgartner, *Chem. Commun.* **2013**, 49, 4899-4901.
- ²³ C. Romero-Nieto, S. Durben, I. M. Kormos, T. Baumgartner, *Adv. Funct. Mater.* **2009**, 19, 3625-3631.
- ²⁴ K. Yamaguchi, T. Murai, J.-D. Guo, T. Sasamori, N. Tokitoh, *ChemistryOpen* **2016**, 5, 434-438.
- ²⁵ Y. Shiraishi, C. Ichimura, S. Sumiya, T. Hirai, *Chem.–Eur. J.* **2011**, 17, 8324-8332.
- ²⁶ S. Achelle, J. Rodríguez-López, N. Cabon, F. Robin-le Guen, *RSC Adv.* **2015**, 5, 107396-107399.
- ²⁷ S. Achelle, J. Rodríguez-López, C. Katan, F. Robin-le Guen, *J. Phys. Chem. C* **2016**, 120, 26986-26995.

- ²⁸ S. Achelle, J. Rodríguez-López, M. Larbani, R. Plaza-Pedroche, F. Robin-le Guen, *Molecules* **2019**, *24*, 1742.
- ²⁹ J. Tydlitát, S. Achelle, J. Rodríguez-López, O. Pytela, T. Mikýsek, N. Cabon, F. Robin-le Guen D. Miklík, Z. Růžicková, F. Bureš, *Dyes Pigm.* **2017**, *146*, 467-478.
- ³⁰ R. S. Hosmane, J. F. Liebman, *Struct. Chem.* **2009**, *20*, 693-697.
- ³¹ P. S. Hariharan, E. M. Mothi, D. Moon, S. P. Anthony, *ACS Appl. Mater. Interfaces* **2016**, *8*, 33034-33042.
- ³² Y. Shen, P. Xue, J. Liu, J. Ding, J. Sun, R. Lu, *Dyes Pigm.* **2019**, *163*, 71-77.
- ³³ J.-J. Vanden Eynde, L. Pascal, Y. Van Haverbeke, P. Dubois, *Synth. Commun.* **2001**, *31*, 3167-3173.
- ³⁴ G. N. Lipunova, E. V. Nosova, T. V. Trashakhova, V. N. Charushin, *Russ. Chem. Rev.* **2011**, *80*, 1115-1133.
- ³⁵ R. Lartia, C. Allain, G. Bordeaux, F. Schmidt, C. Fiorini-Debuisschert, F. Charra, M.-P. Teulade-Fichou, *J. Org. Chem.* **2008**, *73*, 1732-1744.
- ³⁶ S. Achelle, J. Rodríguez-López, F. Robin-le Guen, *J. Org. Chem.* **2014**, *79*, 7564-7571.
- ³⁷ H. Detert, V. Schmitt, *J. Phys. Org. Chem.* **2004**, *17*, 1051-1056.
- ³⁸ C. Katan, M. Charlot, O. Mongin, C. Le Droumaguet, V. Jouikov, F. Terenziani, E. Badaeva, S. Tretiak, M. Blanchard-Desce, *J. Phys. Chem. B* **2010**, *114*, 3152-3169.
- ³⁹ C. Reichardt, *Chem. Rev.* **1994**, *94*, 2319-2358.
- ⁴⁰ Y. Yan, K. Xu, Y. Fang, Z. Wang, *J. Org. Chem.* **2011**, *76*, 6849-6855.
- ⁴¹ C. Liu, Q. Ni, J. Qiu, *Eur. J. Org. Chem.* **2011**, 3009-3015.
- ⁴² Gaussian 16, Revision B.01, M. J. Frisch, G. W. Trucks, H. B. Schlegel, G. E. Scuseria, M. A. Robb, J. R. Cheeseman, G. Scalmani, V. Barone, G. A. Petersson, H. Nakatsuji, X. Li, M. Caricato, A. V. Marenich, J. Bloino, B. G. Janesko, R. Gomperts, B. Mennucci, H. P. Hratchian, J. V. Ortiz, A. F. Izmaylov, J. L. Sonnenberg, D. Williams-Young, F. Ding, F.

Lipparini, F. Egidi, J. Goings, B. Peng, A. Petrone, T. Henderson, D. Ranasinghe, V. G. Zakrzewski, J. Gao, N. Rega, G. Zheng, W. Liang, M. Hada, M. Ehara, K. Toyota, R. Fukuda, J. Hasegawa, M. Ishida, T. Nakajima, Y. Honda, O. Kitao, H. Nakai, T. Vreven, K. Throssell, J. A. Montgomery, Jr., J. E. Peralta, F. Ogliaro, M. J. Bearpark, J. J. Heyd, E. N. Brothers, K. N. Kudin, V. N. Staroverov, T. A. Keith, R. Kobayashi, J. Normand, K. Raghavachari, A. P. Rendell, J. C. Burant, S. S. Iyengar, J. Tomasi, M. Cossi, J. M. Millam, M. Klene, C. Adamo, R. Cammi, J. W. Ochterski, R. L. Martin, K. Morokuma, O. Farkas, J. B. Foresman, D. J. Fox, Gaussian, Inc., Wallingford CT, **2016**.

⁴³ C. Adamo, V. Barone, *J. Chem. Phys.* **1999**, *110*, 6158-6170.

⁴⁴ T. Yanai, D. Tew, N. C. Handy, *Chem. Phys. Lett.* **2004**, *393*, 51-57.

⁴⁵ J. Tomasi, B. Mennucci, R. Cammi, *Chem. Rev.* **2005**, *105*, 2999-3093.

⁴⁶ M. Cossi, V. Barone, *Time J. Chem. Phys.* **2001**, *115*, 4708-4717.

⁴⁷ R. Improta, V. Barone, G. Scalmani, M. J. Frisch, *J. Chem. Phys.* **2006**, *125*, 054103.